



HAL
open science

MULTIVARIATE DISTRIBUTION CORRECTION OF CLIMATE MODEL OUTPUTS: A GENERALISATION OF QUANTILE MAPPING APPROACHES

Léonard Deckens, Sylvie Parey, Mathilde Grandjacques, D Dacunha-Castelle

► **To cite this version:**

Léonard Deckens, Sylvie Parey, Mathilde Grandjacques, D Dacunha-Castelle. MULTIVARIATE DISTRIBUTION CORRECTION OF CLIMATE MODEL OUTPUTS: A GENERALISATION OF QUANTILE MAPPING APPROACHES. *Environmetrics*, 2017, 28 (6), pp.e2454. 10.1002/env.2454 . hal-01569043

HAL Id: hal-01569043

<https://hal.science/hal-01569043>

Submitted on 26 Jul 2017

HAL is a multi-disciplinary open access archive for the deposit and dissemination of scientific research documents, whether they are published or not. The documents may come from teaching and research institutions in France or abroad, or from public or private research centers.

L'archive ouverte pluridisciplinaire **HAL**, est destinée au dépôt et à la diffusion de documents scientifiques de niveau recherche, publiés ou non, émanant des établissements d'enseignement et de recherche français ou étrangers, des laboratoires publics ou privés.

1 **MULTIVARIATE DISTRIBUTION CORRECTION OF CLIMATE MODEL**
2 **OUTPUTS: A GENERALISATION OF QUANTILE MAPPING APPROACHES**

3

4 **Multivariate bias adjustment for climate change studies**

5

6 Research article

7

8 L Dekens^{1,2}, S Parey¹, M Grandjacques³, D Dacunha-Castelle⁴

9 1 : EDF Recherche et Développement site de Chatou, MFEE, France

10 2 : Ecole Normale Supérieure de Lyon et université Claude Bernard Lyon 1, France

11 3 : Lianes (Laboratoire d'Intelligence Artificielle pour les Nouvelles Energies), Institut LIST,
12 CEA, Université Paris-Saclay, F-91120, Palaiseau, France

13 4 : Université Paris Sud, Orsay, France

14

15 Corresponding author : S Parey, EDF Recherche et Developpement 6 quai Watier 78401
16 Chatou France, sylvie.parey@edf.fr

17

18

19 **Abstract:** Climate change impact studies necessitate the estimation of climate variables
20 evolution in the future. These are given by climate model simulations made under different
21 greenhouse gas and aerosol emission scenarios agreed at the international level. However
22 climate model outputs have biases, especially at the local scale, and need to be corrected against
23 observations. Common bias-correction methods are distribution based and form the well-known
24 quantile mapping approaches. This paper presents a generalization of such techniques to the
25 consideration of multivariate distributions. This approach uses the basic lemma of Lévy-
26 Rosenblatt which allows the transport of a distribution on another one, in every dimension. It
27 needs convenient non parametric estimations of conditional repartitions. The approach is first
28 tested in a controlled framework, by use of statistical simulations, then in the real setting of
29 climate simulation, in the bivariate case. An important issue of these types of distribution
30 corrections is the different kinds of hypotheses of stationarity over a long enough period:
31 stationarity of the link between model and observations whatever the period or stationarity of
32 the change between present and future for model and observations. This choice differentiates
33 approaches like Quantile Mapping and CDFt for example in the univariate framework, and
34 makes them more efficient, in the univariate as well as in the multivariate context, when the
35 data to be corrected best verify the assumed hypothesis.

36 **Keywords:** climate change, statistics, multivariate distributions, bias adjustment

37 1 Introduction

38 Since climate change is now attested (IPCC, 2013), and mitigation still underway, adaptation
39 has to be anticipated in parallel to mitigation. The first step in adaptation is an estimation of the
40 possible consequences of climate change at the scale of human societies and their activities.
41 These estimations are commonly done through impact studies, based for example on specific
42 models run with climatic variables. Observed variables are used to represent current conditions,

43 while climate model outputs are used to project future conditions. Climate models are numerical
44 tools based on physical representations of the dynamics of the components, atmosphere, ocean,
45 ice or land surface, and of their interactions, through physical or biochemical processes.
46 Although such tools are more and more sophisticated, including more and more detailed
47 processes, their outputs may still differ significantly from the local observations commonly
48 used by impact models. Therefore, bias correction and downscaling techniques have become
49 an active area of research in the last decade or so. The approach here, like other quantile
50 mapping approaches, can be used for bias adjustment or bias adjustment and downscaling
51 depending on the spatial scale of the reference dataset. When used with local observations it
52 aims at predicting, in statistical terms, local climate variables using more global data provided
53 by a climate model working at a larger scale.

54 Statistical bias correction methods are widely used to correct the distribution of the climate
55 model variables so that they match that of some local observations. Such techniques are
56 commonly recommended for impact studies (Teutschbein and Seibert, 2012; Gudmundsson et
57 al., 2012; Chen et al., 2013). The most used techniques are the so called quantile mapping
58 approaches (Panofsky and Brier, 1958; Haddad and Rosenfeld, 1997; Wood et al. 2004; Déqué
59 2007; Piani et al. 2010), and their variants like CDFt (Michelangeli et al., 2009). A limitation
60 of such techniques is however that the correction is applied independently to the different
61 variables when more than one climatic variable is needed for an impact study, with the risk of
62 degrading the consistency between them. Recent approaches have been proposed to tackle this
63 caveat, and correct two variables, essentially temperature and rainfall, in a consistent way
64 (Zhang and Georgakakos, 2012; Piani and Hearer, 2012; Li et al., 2014). Vrac and Friederichs,
65 2014 go further and propose an approach, based on the empirical copula (by reordering
66 univariate bias-corrected variables), potentially able to tackle both the inter-variable and spatial
67 consistencies. One issue with the approach is however that it can only reproduce the historical

68 temporal sequencing, which is an important limitation for climate impact studies. Cannon, 2016
69 suggests a methodology based on the correction of the marginal distributions again by quantile
70 mapping with then an iterative scheme to push either the Pearson correlation dependence
71 structure or the Spearman rank correlation dependence structure towards observed values.

72 The approach proposed and tested in this paper is a generalization of the quantile mapping
73 techniques to the correction of multivariate distributions. The chosen setting is the typical
74 problem faced with impact studies: over an historical period, time series of different climate
75 variables are available from both climatic databases and climate model simulations, while for a
76 future period, necessarily, only the climate model time series are available. Then, as climate
77 model outputs have biases compared to the observations, the aim of the correction is to estimate
78 for the future period, specific characteristics of time series at the desired location closer to that
79 of the observations. Then, what is expected is not the precise sequencing in time of the variables,
80 which is not an expected result of climate models, but rather characteristics as their distribution,
81 which are quite invariant for time periods with adequate length, not too long to be able to neglect
82 climate trends but not too short to be able to estimate characteristics like distributions. The
83 methodology will be described in the fully multivariate context, considering p dimensions, but
84 in practice, a dimension larger than 2 means much longer time series for the distribution
85 estimations. This methodology uses as basic trick the transportation of a distribution on \mathbb{R}^p onto
86 another one fixed in advance. This is done by repeated applications of the lemma of Levy –
87 Rosenblatt (Grandjacques 2015, Grandjacques et al. 2015). This approach allows to clarify
88 which kind of stationarities are required and also gives a natural way of making clear which
89 period lengths are concerned by all these approaches.

90 The theory underlying the methodology is presented in section 2, and section 3 explains the
91 estimation choices made. Then, section 4 presents an application in a controlled framework, by
92 use of bivariate Gaussian distributions, in order to evaluate when our bivariate bias-correction

93 is best justified. Bivariate Gaussian distributions are easy to handle, although climate variables
94 are generally not normally distributed. The aim here is only to better understand the involved
95 transformations. Finally, section 5 is devoted to an application to real climate variables, before
96 coming to the conclusion and discussion in section 6.

97 2 Theoretical framework

98 2.1 The problem to be solved

99 As previously exposed, the aim here is to simultaneously bias correct different climatic
100 variables according to available observations. We have then 2 time series with values in \mathbb{R}^p :

- 101 - a time series $(Y_t)_{t \in P_0}$ given over the period $P_0 = (1, \dots, n_0)$ only, and corresponding
102 to the observations
- 103 - a time series (X_t) over a much larger period and given by a numerical climate model
104 simulation for example.

105 The aim is then to obtain for a future period P , later than P_0 , a projection of some characteristics
106 of $(Y_t)_{t \in P}$, based on assumptions made about the link between X and Y . In order to make it easier
107 in the following, we will suppose that P and P_0 are of same length and P corresponds to $P_k =$
108 $\{kn_0 + 1, \dots, (k+1)n_0\}$.

109 The proposed methodology is based on the following assumptions.

110

111 Hypothesis H₁: *for each $k \in \mathbb{N}$, there is a process $X_{k,t}$, restriction of X_t when $t \in P_k$, which*
112 *is stationary and weakly mixing. Similarly, it is supposed that there is a process $(Y_t)_{t \in \mathbb{N}}$*
113 *stationary and weakly mixing, for which $(Y_t)_{t \in P_0}$ is a restriction to the period P_0 .*

114 H₁ allows to deal with the intrinsic non stationarity of the data by selecting long enough periods
115 over which it can reasonably be considered as stationary. If n_0 is large enough, this assumption
116 allows valid estimations for some characteristics such as the distributions of $(Y_t)_{t \in P_0}$ or $(X_{k,t})_{t \in P_k}$
117 for k in \mathbb{N} , since both processes have good ergodic properties. “Large enough” here means

118 sufficiently large to apply the law of large number for the needed estimations but not too large
119 to avoid too strong trend effects. The distributions of $(Y_t)_{t \in P_0}$ and $(X_{k,t})_{t \in P_k}$ are respectively noted
120 F_0 and G_k .

121

122 Hypothesis H_2 : *distributions F_0 and G_k are continuous with densities f_0 and g_k*
123 *respectively, with f_0 and g_k , $k \in \mathbb{N}$ strictly positive on the interior of their support.*

124 H_2 avoids having to take conventions to compute inverse functions for the Cumulative
125 Distributions Functions (CDFs), which we will have to consider in the methodology (in fact
126 there is of course no inverse repartition in dimension > 1 but a set of p one dimensional ones
127 which are defined later using the Levy-Rosenblatt lemma). Such conventions would lead to
128 very complex formulations. If one of the components of Y_t is continuous with the exception of
129 a mass on one point, as is the case for rainfall, what follows can easily be extended to consider
130 such a behavior.

131

132 2.2 Distribution transfer on \mathbb{R}^p

133 Definition: *If F and G are distributions defined on \mathbb{R}^p and verifying H_2 , and U^p the uniform*
134 *distribution on \mathbb{R}^p , product of p uniform distributions on \mathbb{R} , then transferring distribution G to*
135 *F will be defined as an application $T : \mathbb{R}^p \rightarrow \mathbb{R}^p$ such that $T(G) = F$, $T(G)$ being the distribution*
136 *image of G through T .*

137 In what follows T is first defined as an application $T : \mathbb{R}^p \rightarrow \mathbb{R}^p$ and then used as operator on
138 distributions, defined for any borelian set I by $T(G)(I) = G(T_H^{-1}(I))$, H being the distribution of
139 I .

140 The notations used for the conditional distributions and their inverses are the following:

141 If Z is a vector with distribution H on \mathbb{R}^p , $Z = (Z^1, Z^2, \dots, Z^p)$, F_l is the distribution of Z^l and
 142 for each k in $\{2, \dots, p\}$, $F_{k/1, \dots, k-1}(z_1, \dots, z_k)$ is the conditional distribution of Z^k for fixed Z^1, \dots, Z^{k-1} .
 143 Thus,

$$144 \quad F_{k/1, \dots, k-1}(z_1, \dots, z_{k-1}, z_k) = P(Z^k \leq z_k | Z^1 = z_1, \dots, Z^{k-1} = z_{k-1})$$

145 Then the inverse function of each strictly increasing function $h: \mathbb{R} \rightarrow \mathbb{R}$ is noted h^{-1} .

146 The following lemma proven by Paul Lévy and better known as the Rosenblatt lemma
 147 (Grandjaques, 2015, Grandjacques et al., 2015) defines a transfer function for each distribution
 148 H (verifying H_2 in our case) on \mathbb{R}^p . H is used here for genericity and stands for any distribution
 149 as F or G mentioned earlier.

150 Lemma 1: if U is defined as

$$151 \quad \begin{cases} U^1 = H_1(Z^1) \\ U^k = H_{k/1, \dots, k-1}(Z^1, \dots, Z^k) \\ U^p = H_{p/1, \dots, p-1}(Z^1, \dots, Z^p) \end{cases}$$

152 then the distribution of $U = (U^k)_{k=1, \dots, p}$ is \mathbf{U}^p , uniform with independent marginal distributions.

153 Thus if T_H is the above described transformation, $T_H(H) = \mathbf{U}^p$ and its inverse $T_H^{-1}: \mathbb{R}^p \rightarrow$
 154 \mathbb{R}^p , such that $T_H^{-1}(\mathbf{U}^p) = H$ is defined as:

$$155 \quad \begin{cases} Z^1 = H_1^{-1}(U^1) \\ Z^k = H_{k/1, \dots, k-1}^{-1}(U^1, \dots, U^k) \\ Z^p = H_{p/1, \dots, p-1}^{-1}(U^1, \dots, U^p) \end{cases}$$

156 Remark: T_H is obviously not the only transformation allowing a distribution transfer, different
 157 versions can be proposed depending for example on the order according to which each

158 component of Z is considered. T_H is sequential with respect to the space dimension; this is a
 159 useful property in the applications. Note that in the Gaussian case it is not at all the classical
 160 transformation obtained by diagonalization of the covariance matrix, which is not sequential.
 161 The analogy is more with a Gramm-Schmidt orthogonalization (Greub, 1975).

162 Lemma 2: transfer of G onto F

163 If $T_{G,F} = T_F^{-1}(T_G)$ then $T_{G,F}$ transfers the distribution G onto the distribution F , because
 164 $T_G(G) = \mathcal{U}$ and $T_F^{-1}(\mathcal{U}) = F$.

165 2.3 Application to the projection of the distribution of Y over the future period

166 P_k

167 The projection of the distribution of Y_t over the future period P_k relies on another assumption
 168 H_3 complementing H_2 and which relates the dynamics of X and Y .

169 At this stage, different hypotheses concerning time invariance can be made:

170 Hypothesis H_{3-1} : let T_{G_k, F_k} $k \geq 1$ be the transformation transferring the distribution G_k of
 171 $(X_{k,t})$ $t \in P_k$, restriction of X_t over P_k , to that of $(Y_{k,t})$, restriction of Y over P_k , then T_{G_k, F_k} does not
 172 depend on k .

$$173 \quad T_{G_k, F_k} = T_{G, F} \text{ for each } k \text{ in } \mathbb{N}$$

174 Thus:

$$175 \quad T_F^{-1}(T_G) = T_{F_k}^{-1}(T_{G_k}) \quad \text{and} \quad T_{F_k}^{-1} = T_F^{-1}(T_G (T_{G_k}^{-1}))$$

176 and the projection over future period P_k can be obtained through:

$$177 \quad \hat{Y}_{k,t} = T_{F_k}^{-1}(T_{G_k}(X_{k,t})) = T_F^{-1}(T_G(X_{k,t})) \text{ with } k \in \mathbb{N}, t \in P_k$$

178 This hypothesis means that the link between both series is invariant in time or that it does not
 179 depend on trends.

180 For univariate bias-correction, this is the hypothesis leading implicitly to the same estimation
 181 as with the techniques linked to Empirical Quantile Matching (Déqué et al., 2007).

182 Hypothesis H₃₋₂: *The transformation between two periods is the same for the*
 183 *observation and for the climate model*

184 It is therefore quite different from our hypothesis H₃₋₁, which states that the transformation
 185 between X and Y is invariant in time.

186
$$T_{F,Fk} = T_{G,Gk} \text{ for every } k \text{ in } \mathbb{N}$$

187 *Thus:*

188
$$T_F^{-1}(T_{Fk}) = T_G^{-1}(T_{Gk}) \quad \text{and} \quad \hat{Y}_{k,t} = T_G^{-1}(T_{Gk}(Y_{0,t}))$$

189 However, if $Y_{k,t}$ in the future is directly computed from the observations recorded over the
 190 observation period, then it will keep the observed interannual variability, since the distribution
 191 only is corrected. Thus to avoid this unrealistic behavior, because there is no reason that
 192 interannual variability in the future will mimic that of the recent past period, one can rather
 193 compute:

194
$$T_{Fk} = T_F(T_G^{-1}(T_{Gk}))$$

195 *and the desired bias corrected time series over future period P_k can be obtained through:*

196
$$\hat{Y}_{k,t} = (T_{Fk})^{-1}(T_{Gk}(X_{k,t})) = (T_{Gk})^{-1}(T_G(T_F^{-1}(T_{Gk}(X_{k,t})))) \quad \text{with } k \in \mathbb{N},$$

197 $t \in P_k$

198 For univariate bias correction, this estimation is the same as the one obtained by the CDFt
 199 correction for example (Cumulative Distribution Function transform, Michelangeli et al.,
 200 2009).

201 We use both approaches in the generalization to multivariate bias correction.

202 H_1 means that the distributions are stationary over long enough periods P_k . H_3 hypotheses mean
 203 either that the link between the deformations of the distributions of the modeled time series X_t
 204 and of the observed ones Y_t over these periods of stationarity does not vary over time (H_{3-2}), or
 205 that the link between the distributions of X_t and Y_t does not depend on time t (H_{3-1}). But, as H_3
 206 only concerns instantaneous distributions, it does not imply the transfer of the entire dynamic
 207 from one time series to the other. This could be done partially for example if what has been
 208 previously described is not applied to F and G but to the distributions of (Y_{t-1}, Y_t) and (X_{t-1}, X_t) ,
 209 which could be possible according to H_2 . Nevertheless, intuitively, it can be seen that some
 210 trajectory properties will bring additional consistency between F_0 and F_k . For example, if F has
 211 2 components, Y_t^1 and Y_t^2 , such consistency is due to the consideration of the whole temporal
 212 dependency, for example that of Y_t^1 and Y_{t-1}^2 .

213 This justifies the idea proposed by different authors (Vrac and Friederich, 2014) of reordering
 214 the time series $Y_{k,t}$, $k \in \mathbb{N}$, $t \in P_k$ with regard to Y_t , $t \in P_0$. Remaining in dimension 2, if

215 $R_t = (r_t^1, r_t^2)$, $t \in P_0$ is the rank vector computed for each component independently,

216 then the transformations to period P_k are the simple permutations σ^1 , σ^2 such that

$$217 \quad \sigma^1(r_t^1, t \in P_k) = (r_t^1, t \in P_0) \text{ and } \sigma^2(r_t^2, t \in P_k) = (r_t^2, t \in P_0).$$

218 However, this implies that the temporal sequencing of the variables over period P_0 is imposed
 219 to the future period P_k , which means in particular that the interannual variability in the period
 220 P_k remains that of period P_0 . This is a very strong assumption, probably too strong because it is

221 physically very unlikely that this will be the case for climate time series. This is not the case
 222 for two historical periods, and it can be anticipated that climate change will impact not only the
 223 mean, but also the variability, and even the whole dynamics, both daily and interannually.

224 With our proposed approach, we have:

$$225 \quad Y_t = T_F^{-1}(U_t) \text{ for } t \in P_0$$

$$226 \quad Y_{k,t} = T_{Fk}^{-1}(U_{k,t}) \text{ for } t \in P_k, \text{ with:}$$

$$227 \quad U_{k,t} = T_{Fk}(Y_t) \text{ and } V_{k,t} = T_{Gk}(X_t)$$

228 The components of U_t and V_t are independent, which allows reordering and applying the
 229 reordering transformation independently for each component. Such a reordering could be
 230 added, but there is still a strong risk of over fitting. This will not be considered here but rather
 231 left for a forthcoming paper.

232 2.4 Validation

233 Once the estimations have been made using functional estimations described in section 2,
 234 validation is undertaken in the following way.

235 The historical period P_0 is divided into two sub-periods Q_0 and Q_I . Then, Q_0 is used to calibrate
 236 F and G and Q_I is used for validation. If \hat{Y}_t , $t \in Q_I$ is the corrected time series, the aim is to
 237 validate the bias-correction using both hypotheses H_{3-1} and H_{3-2} , then either

$$238 \quad \hat{F}_1^{-1} = T_{F_0}^{-1}(T_{G_0}(G_1^{-1}))$$

239 or

$$240 \quad \hat{F}_1 = T_{F_0}(T_{G_0}^{-1}(G_1))$$

241 F_0 and G_0 being the distribution functions over Q_0 and G_I over Q_I .

242 Validation consists then in comparing \hat{F}_1 to F_I which can be estimated here. If d is a distance
243 between distributions in \mathbb{R}^p , the level of correction will be defined as:

$$244 \quad r = \frac{d(F_1, \hat{F}_1)}{d(F_1, G_1)}$$

245 Then the choice of d may be quite arbitrary. If $H(z) = P(Z^1 \leq z^1, \dots, Z^p \leq z^p)$ is the
246 distribution associated to the distribution H of Z on \mathbb{R}^p , the distance which naturally generalizes
247 the distance on \mathbb{R} for continuous distributions is given by $d(H, K) = \sup_{z \in \mathbb{R}^p} |H(z) - K(z)|$.
248 Under the assumption that H and K have densities φ and ψ , a distance L^p like

$$249 \quad d_p(H, K) = \left(\int_{\mathbb{R}^p} |\varphi(z) - \psi(z)|^p \right)^{1/p} \text{ can be used.}$$

250 These distances have been chosen here but others could have been used like the “divergences”
251 proposed by Rust et al, 2010.

252 3 Distribution estimations

253 The distributions F , G and G_k are at first unknown and still to be estimated so that the
254 transformations T_F , T_G and T_{G_k} can be obtained explicitly. This implies the estimation of one
255 dimensional conditional distributions, but with a conditioning on 2 to $p-1$ dimensions.
256 According to hypothesis H_1 and H_2 , all considered distributions have a probability density
257 function on \mathbb{R}^p , which allows the use of non-parametric smoothing methods like kernel density
258 estimation techniques. Two main approaches exist to estimate conditional distributions:

- 259 - direct use of a kernel estimator adjusted through an indicator function (Hall et al.,
260 1999)
- 261 - estimation of a conditional density and integration afterwards (Hyndmann et al.,
262 1996)

263 We will use this last approach, which allows the computation of different validation criteria.
 264 The numerical examples in parts 3 and 4 are given for 2 variables ($p=2$). Even if the theory is
 265 general and valid regardless of the number of dimensions, in practice the number of values
 266 necessary for a reliable estimation of the densities increases in a polynomial way with
 267 dimension p .

268 Let us consider a time series $X_t = (X_t^1, X_t^2)$ which verifies hypotheses H_1 and H_2 . The estimation
 269 of the density of X_t^1 is classical and has good asymptotical properties (for a sufficiently large
 270 number of data) thanks to hypothesis H_1 . This density will be noted $g_1(x^1)$ and its estimator
 271 $\hat{g}_1(x^1)$.

272 Then, $g_{2/1}(x^1, x^2) = \frac{g(x^1, x^2)}{g_1(x^1)}$. The classical kernel density estimator is given by:

$$273 \quad \hat{g}_{2/1}(x^1, x^2) = \frac{\frac{1}{nh^{(1)}h^{(2)}} \sum_{i=1}^n K^{(1)}\left(\frac{x^1 - X_i^1}{h^{(1)}}\right) K^{(2)}\left(\frac{x^2 - X_i^2}{h^{(2)}}\right)}{\frac{1}{nh^{(1)}} \sum_{i=1}^n K^{(1)}\left(\frac{x^1 - X_i^1}{h^{(1)}}\right)}$$

274 where the kernels $K^{(1)}$ and $K^{(2)}$ are positive functions $\mathbb{R} \rightarrow \mathbb{R}$, with integral 1 and whose square
 275 can be integrated. The smoothing parameters $h^{(1)}$ and $h^{(2)}$ are chosen according to the data used
 276 for the estimation.

277 Different types of kernels are generally used:

- 278 - Gaussian: $K(x) = \frac{1}{\sqrt{2\pi}} \exp\left(-\frac{x^2}{2}\right)$,
- 279 - Epanechnikov: $K(x) = \frac{3}{4} (1 - x^2) 1_{\{|x| \leq 1\}}$,
- 280 - Student: $\frac{1}{\sqrt{\pi}} \frac{\Gamma((\nu+1)/2)}{\Gamma(\nu/2)} \left(1 + \frac{x^2}{\nu}\right)^{-\frac{\nu+1}{2}}$

281 We have chosen the Gaussian kernel.

282 To estimate parameters $h^{(1)}$ and $h^{(2)}$ we use the R package “hdcde” developed by R. Hyndmann
283 and based on the methods described in Hyndmann et al., 1996, Bashtannyck and Hyndmann,
284 2001, Hall et al., 1999, Fan et al., 1996, De Gooijer and Gannoun, 2000, Liebscher, 1996 and
285 Hyndmann and Yao, 2002, valid under hypotheses H_1 and H_2 . The choice of $h^{(1)}$, $h^{(2)}$ is then
286 made either by using asymptotical results based on H_2 to which a condition C^2 (stating that all
287 partial derivatives of g have to be twice continuously differentiable) has to be added, or by
288 cross-validation using blocks in order to deal with the weak dependence. The criterion to be
289 minimized in order to choose $h^{(1)}$ and $h^{(2)}$ is generally the L^2 norm between the densities and
290 their estimates. We have also used methods based on sub-sampling and regression (Hall et al.,
291 1999) or kernels with polynomial weights (Bashtannyck and Hyndmann, 2001), and in practice,
292 the approach used in the R package “hdcde” (which mixes regression and sub-sampling for
293 kernel estimation Hyndmann et al., 1996, Bashtannyck and Hyndmann, 2001, Hyndmann and
294 Yao, 2002) is efficient, that is easy to handle and giving good results in a reasonable computing
295 time.

296 4 When is it justified?

297 The previously described methodology aims at bias-correcting the joint distribution of 2 or
298 more variables at the same time. This brings more complexity and needs more data than the
299 usual univariate distribution correction. Thus, in order to judge if there are best suited conditions
300 for the use of such a technique, it has been decided to first test the approach with statistically
301 simulated data.

302 4.1 Design of the simulation study

303 Since shuffling is not considered here, the corrections are only based on the distribution of the
304 data. So, it has been decided to test the approach with data generated by chosen parametric
305 distributions.

306 The aim is thus to simulate 4 bivariate distributions:

- 307 - 1 corresponding to the observations over the current period: F_0
- 308 - 1 corresponding to the model simulation over the same current period: G_0
- 309 - 1 corresponding to the model simulation over a future period: G_k
- 310 - 1 corresponding to the observations over a future period, which is not known a
311 priori and only used to validate the approach: F_k

312 It has been decided to simulate bivariate Gaussian distributions, which is a simple design.

313 4.2 Design of the tests

314 The parameters for the bivariate Gaussian distribution of the current period observations F_0
315 have been chosen based on summer temperature distributions for 2 distant points in Europe,
316 chosen arbitrarily as Hamburg and Orly. The means, variances and co-variances are estimated
317 from the EOBS daily mean temperature time series over the period 1979-2014 for the month of
318 July:

$$319 \quad m_1 = 17.5 \quad m_2 = 20.0 \quad v_{11} = 10 \quad v_{22} = 9 \quad v_{12} = v_{21} = 6$$

320 with m_1 and m_2 respectively the means for variables 1 and 2, v_{11} and v_{22} their variances and v_{12}
321 their co-variance. This leads to a linear correlation $\rho = 0.63$ between both variables.

322 The values corresponding to the observations over current period are thus simulated by a
323 bivariate Gaussian distribution with the above mentioned parameters and 2000 values are
324 produced.

325 Then, some hypotheses have to be made to simulate the data for the model simulations (current
326 and future periods) and for the observations over future period used for verification.

327 To do so, model errors have first been postulated, additive for the means and multiplicative for
328 the variances and co-variances, noted em_1 and em_2 for the mean errors and es_{11} , es_{22} and es_{12}

329 for the variance, co-variance errors. The data corresponding to the model simulations for each
 330 variable over current period (2000 values) are thus produced by a bivariate Gaussian
 331 distribution G_0 with parameters:

$$332 \quad m_1+em_1 \quad m_2+em_2 \quad v_{11} \times es_{11} \quad v_{22} \times es_{22} \quad v_{12} \times es_{12} (=v_{21} \times es_{21})$$

333 Then, climate shifts due to climate change are postulated in the same way, that is as additive
 334 for the means and multiplicative for the variances and co-variances, and noted $dm_1, dm_2, ds_{11},$
 335 ds_{22} and ds_{12} respectively. The 2000 values corresponding to the model simulation over future
 336 period are produced by a bivariate Gaussian distribution G_k with parameters:

$$337 \quad m_1+em_1+dm_1; m_2+em_2+dm_2; v_{11} \times es_{11} \times ds_{11}; v_{22} \times es_{22} \times ds_{22}; v_{12} \times es_{12} \times ds_{12}$$

338 and the data corresponding to the observations over future period (2000 values) are produced
 339 by a bivariate Gaussian distribution F_k with parameters:

$$340 \quad m_1+dm_1 \quad m_2+dm_2 \quad v_{11} \times ds_{11} \quad v_{22} \times ds_{22} \quad v_{12} \times ds_{12} (=v_{21} \times ds_{21})$$

341 The validation criterion is the ratio r defined in section 1.4 with both L_1 and L_∞ norms, which
 342 is the distance between bias-corrected and observed distributions divided by the distance
 343 between simulated and observed distributions, both estimated over the future period.

344 The aim of the applied bias corrections, either univariate or bivariate, is to estimate the bivariate
 345 distribution of the observations for a future period (\hat{F}_k) from that of the observations and model
 346 simulation over current period (F_0 and G_0) and of model simulation over future period (G_k).
 347 Then, the previously defined ratio r measures the performance of the correction in making the
 348 corrected distribution closer to that of the observations over future period F_k than was the
 349 distribution of the model simulation over future period G_k if $r < 1$.

350 Six bias corrections are applied and compared:

- 351 - each variable is independently corrected under hypothesis H_{3-1} (stationarity of the
- 352 transformation between model and observations)
- 353 - each variable is independently corrected under hypothesis H_{3-2} (stationarity of the
- 354 transformation between present and future periods)
- 355 - bivariate correction under hypothesis H_{3-1} with variable 1 corrected first
- 356 - bivariate correction under hypothesis H_{3-1} with variable 2 corrected first
- 357 - bivariate correction under hypothesis H_{3-2} with variable 1 corrected first
- 358 - bivariate correction under hypothesis H_{3-2} with variable 2 corrected first

359 denoted respectively UH, UV, B12H, B21H, B12V, B21V.

360 UH and UV are similar to empirical quantile mapping and CDFt respectively. Here since we
361 only deal with distributions, the bivariate distribution correction under hypothesis H_{3-2} is
362 computed directly from Y_0 through $T_G^{-1}(T_{G_k})$. The univariate bias corrections are computed in
363 the same way as the correction of the first variable in the bivariate corrections, and not taken
364 from the R packages for Quantile Mapping or CDFt, in order to remain consistent in the
365 comparisons.

366 Two cases have been considered in order to better discriminate hypotheses H_{3-1} and H_{3-2} and
367 the consequences of using a correction technique which may not be the best adapted. As a
368 matter of fact, when dealing with climate model simulations, it is difficult to test which
369 stationarity is best verified (because we do not have the observations in the future), and Quantile
370 Mapping or CDFt are generally indifferently used. The chosen cases correspond to:

- 371 - one case with model errors larger than climate change
- 372 - one case with climate change larger than model errors

373 In order to be able to test the order of variable corrections in the bivariate corrections, the errors
374 and climate change shifts are not equal for each variable. The test cases are made with:

- 375 - $em_1=4; em_2=5; es_{11}=es_{22}=es_{12}= 0.5$ and $dm_1=2; dm_2=1.5; ds_{11}=ds_{22}=1.2 ; ds_{12}= 1$
376 - $em_1=1; em_2=1.5; es_{11}=0.8 ;es_{22}=0.75 ;es_{12}= 0.9$ and $dm_1=4; dm_2=5; ds_{11}=ds_{22}=1.5;$
377 $ds_{12}= 1$

378 The choices have been made in considering observed model errors and climate change changes:
379 climate models tend to underestimate the variances and in summer, both the means and the
380 variances increase. Then this behavior has been exaggerated to produce large errors and large
381 climate shifts.

382 4.3 Results

383 As previously described, we first simulate 2000 values with Gaussian bivariate distributions
384 using fixed means and variances/co-variances, from which we then non-parametrically estimate
385 bivariate distributions to compute distances and compare the different bias corrections. The
386 non-parametrical estimation is based on the R function “kde2d” of package MASS, and with
387 2000 values only, such an estimation is uncertain. It has thus first been verified that the distances
388 between the bivariate distributions with the chosen errors and climate change shifts are
389 significantly larger than the distances between 2 sets of 2000 points taken from the same
390 distribution. This is preferred to the consideration of a much larger number of values, because
391 firstly, this considerably increases computing time for the corrections and secondly, in climate
392 change studies, when corrections have to be made it is generally done on a monthly basis, we
393 do not dispose of much more values. Thus 4 sets of 2000 points are produced by use of a
394 bivariate Gaussian distribution: one mimicking 2 variables as observed under current climate
395 conditions, another for current climate as simulated by a climate model and the 2 other sets
396 mimicking observed and modeled variables under future climate conditions. Then the
397 previously defined 6 bias corrections are applied to the set corresponding to the modeled
398 variables under future climate conditions so that its distribution gets closer to that of the

399 variables corresponding to the observed ones under future climate conditions (as we are here in
 400 an academic situation where all 4 distributions are simulated). This is done 30 times and the
 401 distributions of the r ratios are examined.

402 4.3.1 Errors larger than climate change

403 In order to test for the best suited stationarity hypothesis, the transformations based on
 404 hypotheses H_{3-1} and H_{3-2} are applied to the same sample. H_{3-1} states that $T_F^{-1}(T_G) = T_{F_k}^{-1}(T_{G_k})$
 405 thus both $T_F^{-1}(T_G)$ and $T_{F_k}^{-1}(T_{G_k})$ are applied to the sample obtained with G_0 . Then, the distance
 406 between the obtained distributions is computed (as L_1 or L_∞ norm). Similarly, H_{3-2} postulates
 407 that $T_F^{-1}(T_{F_k}) = T_G^{-1}(T_{G_k})$ thus both $T_F^{-1}(T_{F_k})$ and $T_G^{-1}(T_{G_k})$ are applied to the sample obtained
 408 with F_0 and the distance between the obtained distributions is computed. Each transformation
 409 is computed with variable 1 first and with variable 2 first, and 30 generations are considered.
 410 Then, the distance corresponding to H_{3-1} is compared to that corresponding to H_{3-2} to infer the
 411 best verified hypothesis. In this case, the average L_1 distances corresponding to each
 412 transformation for the 30 tests are as follows:

413	distance according to H_{3-1} with variable 1 first:	$6.2 \cdot 10^{-4}$
414	distance according to H_{3-1} with variable 2 first:	$6.3 \cdot 10^{-4}$
415	distance according to H_{3-2} with variable 1 first:	$7.5 \cdot 10^{-4}$
416	distance according to H_{3-2} with variable 2 first:	$8.4 \cdot 10^{-4}$

417 The distances after H_{3-1} are lower, so hypothesis H_{3-1} seems best verified. Each of the six
 418 corrections are then applied to estimate F_k and figure 1 presents the boxplots of the r ratio for
 419 each correction using either L_1 (top panel) or L_∞ (bottom panel) distances. It shows that, as
 420 expected, both univariate and bivariate corrections based on hypothesis H_{3-1} (UH, B12H and
 421 B21H) perform better than those based on hypothesis H_{3-2} (UV, B12V and B21V), although

422 these last corrections bring some improvement too. In this case, the correction is very efficient
423 (mean ratios around 0.2) and the bivariate correction does not bring substantial improvement.

424 4.3.2 Climate change larger than model errors

425 In this case, the mean distances between the different transformations are as follows:

426 distance according to H_{3-1} with variable 1 first: $6.5 \cdot 10^{-4}$

427 distance according to H_{3-1} with variable 2 first: $8.2 \cdot 10^{-4}$

428 distance according to H_{3-2} with variable 1 first: $2.9 \cdot 10^{-4}$

429 distance according to H_{3-2} with variable 2 first: $3.6 \cdot 10^{-4}$

430 Hypothesis H_{3-2} is here best verified. Again, the obtained results after applying each of the six
431 distribution corrections (figure 2) confirm that the corrections based on hypothesis H_{3-2} perform
432 better in this case. The corrections are however much less efficient than in the previous setting,
433 with best ratios around 0.5 while they were around 0.2 in the previous case, but this may be due
434 to the chosen parameters. Actually, the choices made for the model errors and climate change
435 shifts are not symmetrical. Here, choosing the least verified hypothesis may lead to ratios higher
436 than 1 (no corrections). Here, bivariate correction, at least when starting with variable 1, brings
437 some improvement compared to independent univariate corrections.

438 In both cases, the improvements due to the most suited correction appear more clearly with
439 distance L_∞ . Distance L_1 is an average over the whole distribution (or at least its estimation on
440 some grid) while distance L_∞ corresponds to a single value: the maximal one. As here, the
441 introduced errors imply distribution shifts, the corrections reduce the shift and thus have a
442 greater impact on L_∞ than on L_1 .

443 4.3.3 The role of correlation strength

444 Another question arising in this context is the role of the correlation strength between the
445 variables in the importance and performance of multivariate bias correction. In order to
446 investigate this point, the previous tests have been performed again with lower covariances
447 between both variables:

448 $v_{12}=v_{21}=3$ which leads to a linear correlation coefficient ρ around 0.3

449 $v_{12}=v_{21}=1$ which leads to a linear correlation coefficient ρ around 0.1

450 respectively called medium and low correlation, while the previous test is called high
451 correlation. The results are presented for L_1 and L_∞ norms in figure 3, in keeping only the best
452 corrections in each case (H for hypothesis H_{3-1} in the case of larger model errors than climate
453 shifts and V for hypothesis H_{3-2} in the reverse case). They show that the correlation strength
454 does not have any significant impact on the performance of the corrections, even though, in the
455 case of climate shifts larger than model errors, bivariate correction performs better than
456 univariate correction in the strong correlation case but equally well otherwise. Correlation has
457 been compared too (figure 4). While univariate correction does not really change the model
458 correlation, bivariate correction does, and generally in the right way. However, bivariate
459 correction seems to underestimate the correlation coefficient when covariance (and correlation)
460 is high, especially when hypothesis H_{3-2} is concerned. Moreover, bivariate correction shows
461 more variable results than univariate correction among the 30 bivariate Gaussian distribution
462 generations. This is most probably due to the fact that bivariate correction needs more
463 distribution estimations than univariate correction, which increases statistical errors.

464 Now, when both model errors and climate shifts are moderate:

465 $em_1=1$; $em_2=1.5$; $es_{11}=0.8$; $es_{22}=0.75$; $es_{12}=0.9$ and $dm_1=2$; $dm_2=1.5$; $ds_{11}=ds_{22}=1.2$; $ds_{12}=1$

466 then both corrections perform as well, as can be seen in figure 5, because both hypotheses are
467 quite equally verified. However, the dispersion for the bivariate correction is higher again,

468 which may be linked to the uncertainty in the bivariate distribution estimation when the
469 correlation is high. As a matter of fact, with these parameters, the correlation between both
470 variables is 0.63 for F_0 and goes to 0.73 for G_0 . This was the same for the case with higher
471 climate shifts than model errors, which showed a similar behavior (figure 2).

472 5 Test with climate data

473 The goal of the developed approach is the bias-correction of climate data, thus the next step
474 consists in testing it with observed and model variables. As all here is defined for continuous
475 distributions, and in order to test the approach with different distributions for each variable, it
476 has been decided to work with temperature and wind speed. Long time series of observed daily
477 mean temperature and wind speed have been obtained for the city of Hamburg in Germany
478 from the ECA&D project web site (<http://eca.knmi.nl/dailydata/>) (Klein Tank et al., 2002). In
479 order to maximize the chance that the time series are homogeneous, they will be considered
480 from 1950 to 2015 (66 years). Then, the climate model simulation of the IPSL-CM5-MR model
481 (Dufresne et al., 2013) has been arbitrarily chosen in the CMIP5 database as a test model, and
482 the time series of the nearest grid box to Hamburg has been extracted from the historical run
483 (1950-2005) and the RCP 8.5 projection run (2006-2100), to compute time series of daily mean
484 temperature and wind speed over the same period $P_0=1950-2015$. This period is then divided
485 into two 33-year sub-periods, $Q_1=1950-1982$, chosen as calibration period, and $Q_2=1983-2015$
486 chosen as validation period.

487 As the approach is valid for stationary time series over the defined periods, the correction is
488 applied on a monthly basis, in order to get rid of the annual cycle. It is always difficult to
489 consider that climatic variables are stationary over a defined period, because of both climate
490 change and interannual variability. The World Meteorological Organization recommends to
491 consider at least 30 years to define the climate of an area, thus considering 33-year periods
492 seems a reasonable choice.

493 First, the distances after transformations of the same sample according to each H_{3-1} and H_{3-2}
494 hypothesis are computed for each month to infer which one is best verified. Table 1 summarizes
495 the results for each month, together with an indication of the correlation between wind and
496 temperature as observed over period Q_1 according to the linear Pearson correlation coefficient
497 or the rank Spearman one. Except for July, for which H_{3-1} seems clearly best verified, for all
498 other months, either H_{3-1} show a small preference or it is difficult to discriminate both
499 hypothesis. Therefore, the multivariate correction will be applied according to H_{3-1} , which
500 corresponds to estimations similar as those made by Empirical Quantile Mapping, since
501 between 2 recent past periods the climate shift is not too high. Here, the functions of the R
502 package *qmap* have been used for the univariate corrections in order to compare our proposed
503 approach to standard ones used in climate studies. Daily temperature and wind speed are
504 generally moderately correlated (positively in winter, negatively in summer) except in
505 September.

506 5.1 Temperature first, then wind

507 The first test is made by correcting temperature first, and then wind according to temperature
508 as described in sections 1 and 2. The ratios of the distance between the bivariate distribution of
509 the corrected variables and the observed ones divided by the distance between the modeled
510 variables and the observed ones over the validation period are compared for both bivariate and
511 independent univariate bias-corrections for each month (table 2). Here only the L_1 norm is
512 considered as both used norms lead to the same conclusions in the previous section. The first
513 outcome is that, generally bias-correction improves the distance to the observations (ratio <1),
514 and bivariate correction gives slightly better results than univariate corrections for 7 months.
515 The worst correction is obtained for the month of May, while the best occurs in July, both for
516 univariate and bivariate corrections. Figure 6 allows the comparison of the bivariate
517 distributions in May, for observations and model over the calibration (Q_1) and validation (Q_2)

518 periods and for Q_1 and Q_2 for the model and the observations. It shows that the model errors are
519 rather low, and that there is very little change between both periods, for the model as well as
520 for the observations. It is thus not surprising that the correction is modest in this case, as shown
521 in figure 7. On the contrary, in July (figure 8) the model errors are quite large, and climate
522 change is modest. The situation is more similar to that of our academic case with large model
523 errors and moderate climate shift which previously lead to the best corrections based on
524 hypothesis H_{3-1} (section 4.3.1). Figure 9 illustrates the distributions before and after corrections
525 and shows that bivariate correction brings some improvement. As far as correlation is
526 concerned, univariate bias correction does not have any impact on the model correlation,
527 whereas bivariate correction does, and generally improves the correlation. This can be seen in
528 table 2 for example for May, when the model anti-correlation is stronger than observed and this
529 is better after bivariate correction or for July when model anti-correlation is weaker than
530 observed and increased by the bivariate bias correction. This is shown for the Spearman rank
531 correlation coefficient but the results are similar with the Pearson correlation coefficient. Thus
532 bivariate corrections clearly improve the situation if the correlations for observation and model
533 are different enough to allow the correction being larger than the statistical errors due to the
534 dimension.

535 5.2 Wind first then temperature

536 The same corrections have then been tested again but by correcting wind speed first, and then
537 temperature according to wind speed. The ratios of distances after and before correction are
538 summarized in table 3, together with the Spearman rank correlation coefficients. The results are
539 similar even though the months for which univariate correction gives slightly better results are
540 not always the same. July shows again the best performance for the corrections while May
541 remains the worst corrected, with a small advantage to bivariate correction though.

542 6 Conclusion and perspectives

543 In this paper, a new approach for bias-correcting multivariate distributions of climate model
544 simulations according to observations has been proposed and tested in controlled conditions,
545 by use of statistical simulations, and in real conditions, with a climate model simulation and
546 observations for wind speed and temperature. This approach is based on the Lévy-Rosenblatt
547 lemma and generalizes the univariate distribution corrections like empirical quantile mapping
548 or CDFt.

549 The development of the technique first showed that depending on the hypothesis made
550 (invariance of the transformation between model and observations in time or invariance of the
551 transformation between two periods for observed and model variables), the correction is similar
552 to empirical quantile mapping or to CDFt.

553 Then, the tests with bivariate Gaussian distributions allowed to compare the performances of
554 the corrections in controlling the model errors and climate shifts, as well as the strength of the
555 variables correlation. The parameters are based on observed and model July temperature for
556 two distant points, and willingly exaggerated in order to better see the differences in the
557 approaches. It shows that the verification of the chosen stationary hypothesis: H_{3-1} (stationarity
558 of the link between model and observations) or H_{3-2} (stationarity of the link between present
559 end future conditions) has a stronger importance for the correction performance than univariate
560 or bivariate correction, whatever the correlation strength between both variables. Furthermore,
561 the order of variable corrections does not seem to have important consequences in this
562 framework.

563 Then a last test is made in a more real setting, with daily mean temperature and wind speed
564 time series observed over period 1950-2015 and simulated by the IPSL-CM5-MR model in
565 Hamburg. The corrections are applied on a monthly basis, in order to meet as closely as possible
566 the hypothesis of stationarity, in a cross-validation setting, 1950-1982 being the calibration
567 period and 1983-2015 the validation period. Daily temperature and wind speed are moderately

568 correlated in each month, with a positive correlation in winter and a negative one in summer,
569 with lower correlation in fall and spring (and almost no correlation in September). As the
570 periods are close, the conditions of a more reliable application of corrections based on
571 hypothesis H_{3-1} are generally met and this technique is applied. The results show that bivariate
572 correction generally leads to a slightly better correction.

573 This study opens some questions before the application of such a correction can be generalized.
574 First it can be extended to the case of at least one variable with non-continuous distribution.
575 Most applications have to deal with temperature and rainfall rather than temperature and wind
576 speed. Two ways can be tested to do so:

- 577 - Correction of the number of rainy days (based on the differences between model and
578 observations if H_{3-1} is considered or on the change between present and future if H_{3-2}
579 is considered), then of the amount of rainfall on rainy days and finally of
580 temperature according to rainfall (in managing again rainy and non-rainy days)
- 581 - Transformation of the rainfall distribution so that it becomes more continuous as
582 proposed in Vrac et al 2016

583 Then although the methodology is generic and theoretically works regardless of the number of
584 variables, extension to more than two variables will need more data for the estimations to be
585 reliable. Furthermore, the need to estimate more distributions increases the statistical errors and
586 the improvement is more obvious if the discrepancies to be corrected are large.

587 Lastly, the very important question of stationarity remains. Applying the correction on a
588 monthly basis is the easiest solution. However, because of interannual variability, it is necessary
589 to calibrate the correction over a long enough period (at least 30 years). Then in the climate
590 change context, the conditions of application of empirical quantile mapping like approaches
591 (based on hypothesis H_{3-1}), that the distributions are invariant in time, cannot hold, and then,

592 CDFt like approaches (based on hypothesis H_{3-2}) are more adapted, but may bring a lower
593 improvement. Besides, using Quantile Mapping like corrections in such cases may worsen the
594 situation. It seems then important to think at techniques able to stationarize the distributions
595 and let them be closer in time and between observation and model. This can be done by
596 removing seasonalities and trends, at least in the mean and the variance. However, part of the
597 bias is embedded in the estimation of such quantities for the model time series and they have to
598 be corrected too. In a univariate context, this can be made in an additive or multiplicative way.
599 But in a multivariate context, this implies to think at a way of consistently correcting these parts
600 of the signal as well. Future work will consist in clarifying these questions of non stationarity
601 by working with a parameterization of the two kinds of dynamic deformations we have
602 formalized in hypotheses H_{3-1} and H_{3-2} . Such parameterization should be more complex than a
603 simple shift but still simple enough to be applied routinely.

604 **Acknowledgements**

605 *The authors would like to acknowledge funding for the European Climatic Energy Mixes (ECEM) project by the*
606 *Copernicus Climate Change Service, a programme being implemented by the European Centre for Medium-Range*
607 *Weather Forecasts 5 (ECMWF) on behalf of the European Commission. The specific grant number is*
608 *2015/C3S_441_Lot2_UEA.*

609

610 7 References

611 Bashtannyk D. M., Hyndmann R. J., 2001: Bandwidth selection for kernel conditional density
612 estimation, *Computational Statistics & Data Analysis*

613 Cannon A. J., 2016: Multivariate Bias Correction of Climate Model Output: Matching Marginal
614 Distributions and Intervariable Dependence Structure. *Journal of Climate*, 29, 7045-7064, DOI:
615 10.1175/JCLI-D-15-0679.1

616 Chen J., Brissette F. P., Chaumont D., and Braun M., 2013: Finding appropriate bias correction
617 methods in downscaling precipitation for hydrologic impact studies over North America. *Water*
618 *Resources Research*, 49 (7), 4187–4205, doi:10.1002/wrcr.20331

619 De Gooijer J.G. and Gannoun A., 2000: Nonparametric conditional predictive regions for time
620 series, *Computational Statistics and Data Analysis* 33, 259–275.

621 Déqué M., 2007: Frequency of precipitation and temperature extremes over France in an
622 anthropogenic scenario: Model results and statistical correction according to observed values,
623 *Global Planet. Change*, 57, 16– 26

624 Dufresne J-L, Foujols M-A, Denvil S, Caubel A, Marti O, Aumont O, Balkanski Y, Bekki S,
625 Bellenger H, Benschila R, Bony S, Bopp L, Braconnot P, Brockmann P, Cadule P, Cheruy F,
626 Codron F, Cozic A, Cugnet D, de Noblet N, Duvel J-P, Ethé C, Fairhead L, Fichefet T, Flavoni
627 S, Friedlingstein P, Grandpeix J-Y, Guez L, Guilyardi E, Hauglustaine D, Hourdin F, Idelkadi
628 A, Ghattas J, Joussaume S, Kageyama M, Krinner G, Labetoulle S, Lahellec A, Lefebvre M-P,
629 Lefevre F, Levy C, Li ZX, Lloyd J, Lott F, Madec G, Mancip M, Marchand M, Masson S,
630 Meurdesoif Y, Mignot J, Musat I, Parouty S, Polcher J, Rio C, Schulz M, Swingedouw D, Szopa
631 S, Talandier C, Terray P, Viovy N, Vuichard N, 2013: Climate change projections using the
632 IPSLCM5 earth system model: from CMIP3 to CMIP5. *Climate Dynamics* 40(9):2123–2165

633 Fan J., Yao Q and Tong H., 1996: Estimation of conditional densities and sensitivity measures
634 in nonlinear dynamical systems. *Biometrika*, 83 (1). pp. 189-206.

635 Grandjacques, M., 2015 : Analyse de sensibilité pour des modèles stochastiques à entrées
636 dépendantes : application en énergétique du bâtiment. Thèse Université de Grenoble

637 Grandjacques M., Delinchant B., Adrot O. Pick and Freeze, 2015: estimation of sensitivity
638 index for static and dynamic models with dependent inputs - hal.archives-ouvertes.fr

639 Greub W. H., 1975: Linear Algebra, 4th edition, Springer Verlag

640 Gudmundsson L., Bremnes J., Haugen J., and Engen-Skaugen T., 2012: Technical note:
641 Downscaling RCM precipitation to the station scale using statistical transformations—a
642 comparison of methods. *Hydrology & Earth System Sciences*, 16 (9), 3383–3390,
643 doi:10.5194/hess-16-3383-2012

644 Haddad, Z. and D. Rosenfeld, 1997: Optimality of empirical z-r relations. *Q. J. R. Meteorol.*
645 *Soc.*, 123, 1283-1293

646 Hall P, Wolff R, Yao Q, 1999: Methods for estimating a conditional distribution function,
647 *Journal of the American Statistical Association*, 94 (445). pp. 154-163

648 Hyndmann R, Bashtannyk D M, Grunwald G K, 1996: Estimating and visualizing conditional
649 densities, *Journal of Computational and Graphical Statistics*, 1996

650 Hyndmann R, Yao Q, 2002: Nonparametric estimation and symmetry test for conditional
651 density functions, *Nonparametric statistics*

652 IPCC, “Climate change 2013; The physical basis - summary for policymakers,” Fifth
653 Assessment Report of the Intergovernmental Panel on Climate Change, 2013

654 Klein Tank, A. M. G., et al., 2002: Daily dataset of 20th-century surface air temperature and
655 precipitation series for the European Climate Assessment, *International Journal of Climatology*,
656 22, 1,441–1,453, Data and metadata available at <http://eca.knmi.nl>.

657 Liebscher E., 1996: Strong convergence of sums of c-mixing random variables with
658 applications to density estimation. *Stochastic Processes and their Applications* 65

659 Li C., Sinha E., Horton D.E., Diffenbaugh N.S., and Michalak A.M., 2014: Joint bias correction
660 of temperature and precipitation in climate model simulations. *Journal of Geophysical*
661 *Research: Atmospheres*, 119 (23), 13–153, doi:10.1002/2014JD022514

662 Michelangeli P.-A., Vrac M., and Loukos H., 2009: Probabilistic downscaling approaches:
663 Application to wind cumulative distribution functions, *Geophys. Res. Lett.*, 36, L11708,
664 doi:10.1029/2009GL038401

665 Panofsky H. and Brier G., 1958: Some applications of statistics to meteorology. Tech. rep.,
666 University Park, Penn. State Univ., 224 pp

667 Piani, C., Haerter J., and Coppola E., 2010: Statistical bias correction for daily precipitation in
668 regional climate models over Europe. *Theoretical and Applied Climatology*, 99, 187-192,
669 doi:10.1007/s00704-009-0134-9

670 Piani, C. and Haerter J.O., 2012: Two dimensional bias correction of temperature and
671 precipitation copulas in climate models. *Geophys. Res. Lett.*, doi:10.1029/2012GL053839

672 Rust H., Vrac M., Lengaigne M., Sultan B.: Quantifying Differences in Circulation Patterns
673 Based on Probabilistic Models. *J. Climate*, 23:6573-6589, 2010

674 Teutschbein, C., and Seibert J., 2012: Bias correction of regional climate model simulations for
675 hydrological climate-change impact studies: Review and evaluation of different methods.
676 *Journal of Hydrology*, 456, 12–29, doi:10.1175/JAMC-D-11-0149.1

677 Vrac, M. and Friederichs P., 2015: Multivariate-intervariable, spatial, and temporal-bias
678 correction. *Journal of Climate*, 28 (1), 218–237, doi:10.1175/JCLI-D-14-00059.1

679 Wood A., Leung L., Sridhar V. and Lettenmaier D., 2004: Hydrologic implications of
680 dynamical and statistical approaches to downscaling climate model outputs. *Clim. Change*, 62
681 (189-216).

682 Vrac M., Noël T., Vautard R., 2016 : Bias correction of precipitation through Singularity
683 Stochastic Removal: Because occurrences matter. *Journal of Geophysical Research*
684 *Atmosphere*, doi: 10.1002/2015JD024511

685 Zhang F., and Georgakakos A.P., 2012: Joint variable spatial downscaling. *Climatic Change*,
686 111 (3-4), 945–972, doi:10.1007/s10584-011-0167-9

687

688

689

TABLES

690

Month	H ₃₋₁	H ₃₋₁ w	H ₃₋₂	H ₃₋₂ w	correlation			
	T first	first	T first	first	observations		IPSL simulation	
	L ₁ (10 ⁻⁴)	L ₁ (10 ⁻⁴)	L ₁ (10 ⁻⁴)	L ₁ (10 ⁻⁴)	Pearson	Spearman	Pearson	Spearman
January	7.0	6.6	9.5	9.0	0.47	0.50	0.50	0.54
February	7.0	6.3	10.5	8.1	0.36	0.35	0.40	0.43
March	14.7	13.2	14.0	13.8	0.11	0.10	0.17	0.18
April	18.0	17.1	17.1	17.3	-0.15	-0.15	-0.07	-0.06
May	13.7	12.6	19.0	17.6	-0.17	-0.17	-0.32	-0.33
June	21.5	20.8	21.6	21.3	-0.28	-0.28	-0.27	-0.26
July	13.2	12.2	26.2	28.5	-0.37	-0.39	-0.19	-0.15
August	15.0	16.2	17.3	20.0	-0.21	-0.22	-0.32	-0.30
September	14.5	14.8	19.3	22.9	-0.01	0.00	-0.14	-0.13
October	13.3	9.6	10.5	9.3	0.17	0.16	0.10	0.11
November	8.2	11.6	12.2	13.3	0.33	0.33	0.39	0.40
December	9.4	8.7	11.7	11.2	0.46	0.48	0.47	0.50

691 Table 1: L₁ distance between the bivariate distributions obtained with transformations based
692 on hypothesis H₃₋₁ with temperature (T) or wind (w) first (first two columns) and between the
693 bivariate distributions obtained with transformations based on hypothesis H₃₋₂ with
694 temperature (T) or wind (w) first (columns 3 and 4), correlation between temperature and
695 wind (Pearson and Spearman coefficients for the observations (columns 6 and 7) and for the
696 IPSL model simulation (columns 8 and 9) for each month

697

Month	correlation		Bivariate correction		Univariate correction	
	observations	IPSL model	Distance ratio	correlation	Distance ratio	correlation
January	0.55	0.55	0.522	0.62	0.563	0.55
February	0.44	0.43	0.328	0.39	0.301	0.43
March	0.11	0.18	0.758	0.17	0.771	0.18
April	-0.08	-0.05	0.713	-0.14	0.712	-0.05
May	-0.11	-0.30	0.992	-0.21	1.098	-0.30
June	-0.26	-0.29	0.496	-0.33	0.483	-0.29
July	-0.31	-0.16	0.179	-0.40	0.244	-0.16
August	-0.20	-0.34	0.600	-0.36	0.606	-0.34
September	0.05	-0.12	0.855	-0.03	0.845	-0.12
October	0.15	0.12	0.934	0.17	0.952	0.12
November	0.32	0.36	0.788	0.36	0.849	0.36
December	0.49	0.47	0.671	0.45	0.650	0.47

699 Table 2: correlation (Spearman rank correlation coefficient) over the validation period and
700 ratio of the distance (between the bivariate distributions of the corrected and observed
701 variables divided by that of the modeled and observed variables) and correlation over the
702 validation period after bivariate bias correction with temperature corrected first and
703 independent univariate bias-correction. Bold indicates the lowest ratios obtained when
704 correction is efficient

705

706

Month	correlation		Bivariate correction		Univariate correction	
	observations	IPSL model	Distance ratio	correlation	Distance ratio	correlation
January	0.55	0.55	0.532	0.48	0.563	0.55
February	0.44	0.43	0.316	0.33	0.301	0.43
March	0.11	0.18	0.729	0.12	0.771	0.18
April	-0.08	-0.05	0.695	-0.11	0.712	-0.05
May	-0.11	-0.30	0.968	-0.19	<i>1.098</i>	-0.30
June	-0.26	-0.29	0.523	-0.35	0.483	-0.29
July	-0.31	-0.16	0.196	-0.39	0.244	-0.16
August	-0.20	-0.34	0.571	-0.36	0.606	-0.34
September	0.05	-0.12	0.853	-0.09	0.845	-0.12
October	0.15	0.12	0.970	0.19	0.952	0.12
November	0.32	0.36	0.819	0.30	0.849	0.36
December	0.49	0.47	0.601	0.58	0.650	0.47

707 Table 3: same as table 2 but for wind corrected first, then temperature according to wind

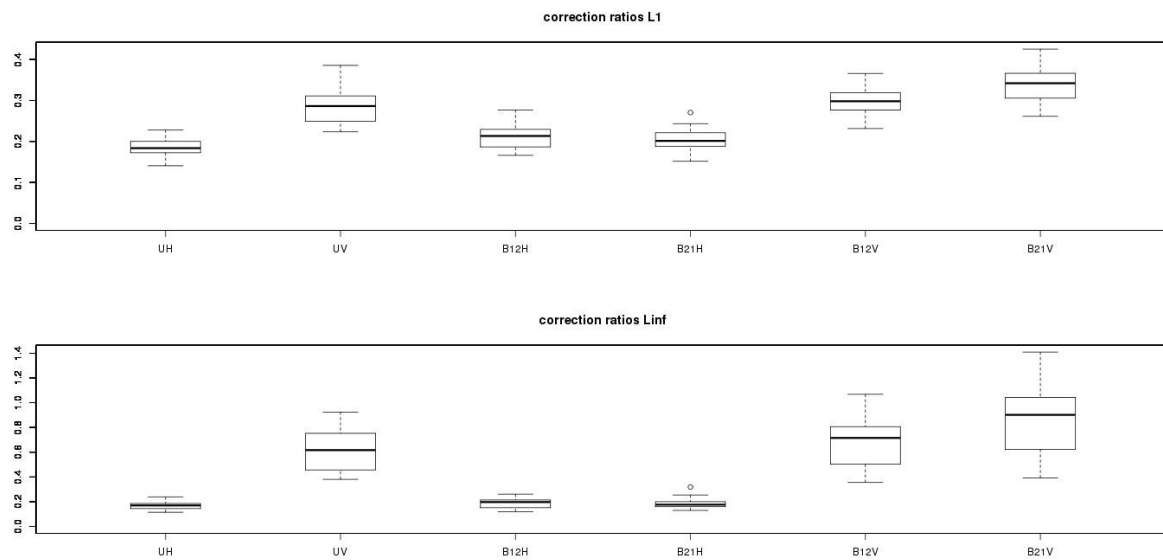
708

709

710

FIGURES

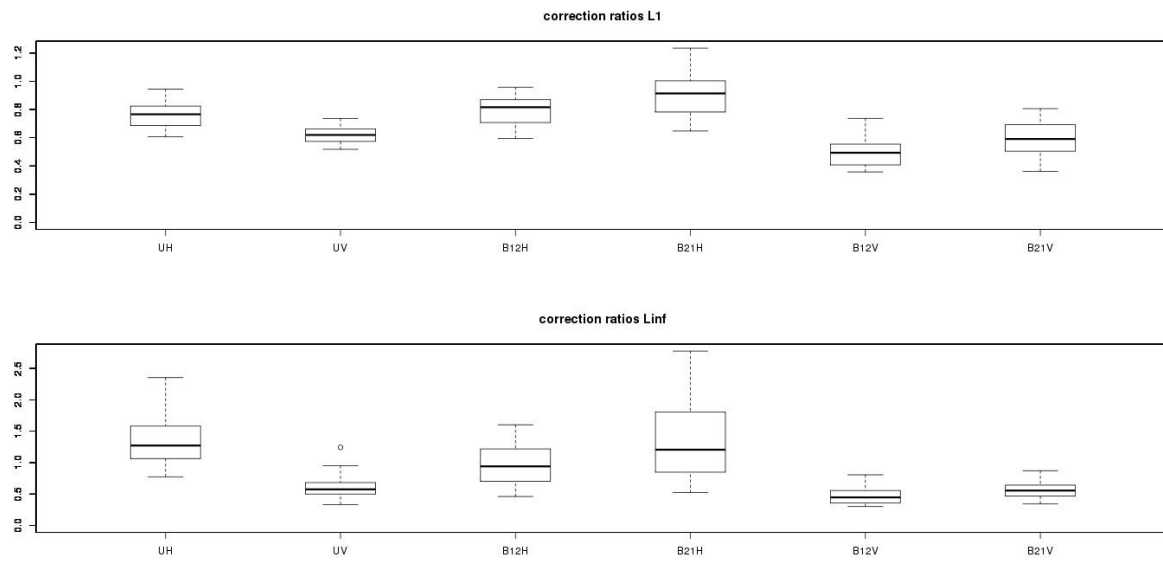
711



712

713 Figure 1: boxplots of the correction ratios obtained with 30 simulations with bivariate
714 Gaussian distributions in the case of larger model errors than climate shifts, based on distance
715 L_1 (top panel) and L_∞ (bottom panel). U refers to univariate correction, B to bivariate starting
716 by variable 1 (12) or 2 (21) and H is for hypothesis H_{3-1} and V for hypothesis H_{3-2}

717



719

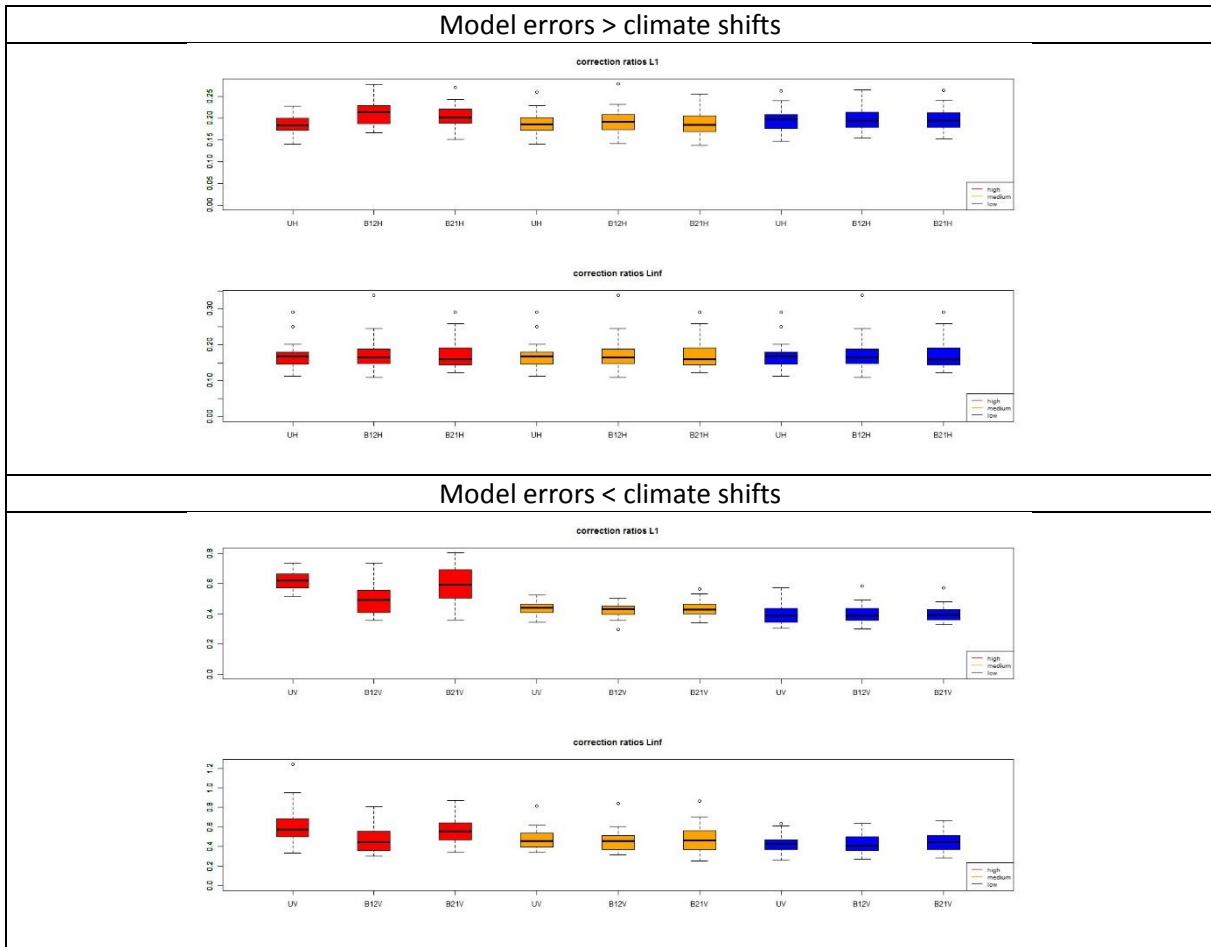
720

721 Figure 2: boxplots of the correction ratios obtained with 30 simulations with bivariate

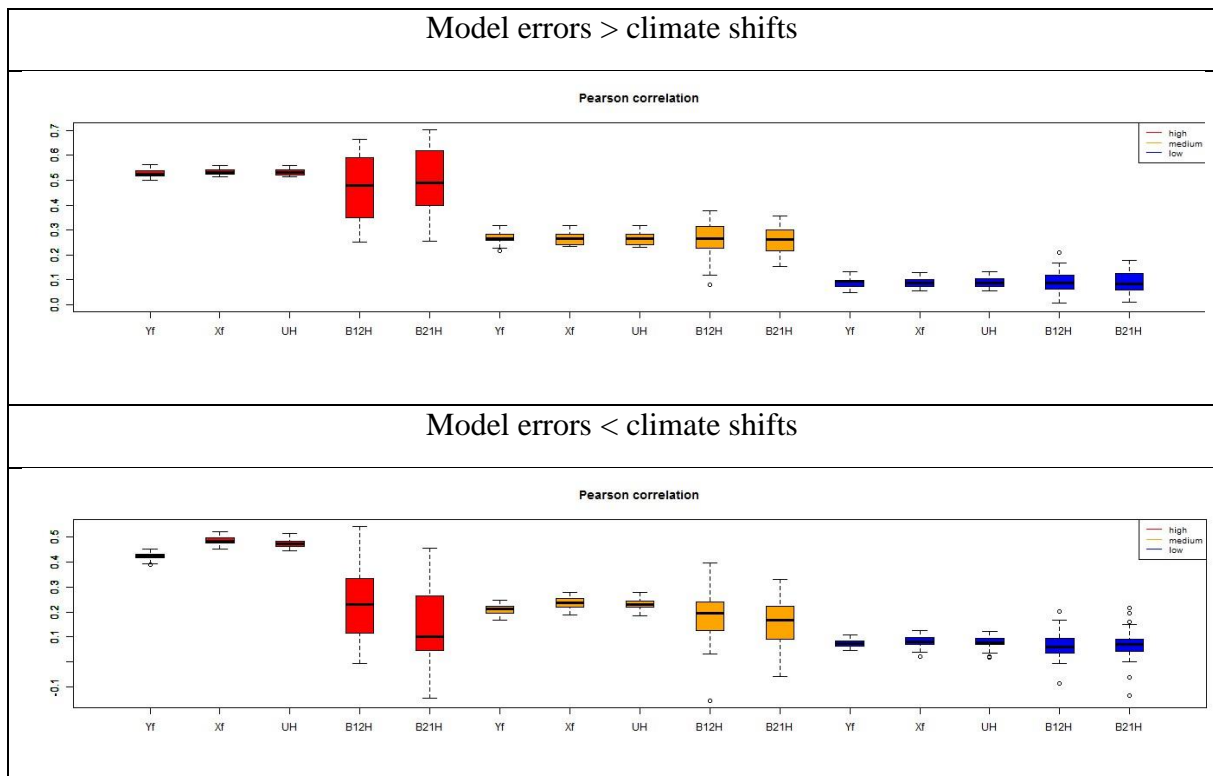
722 Gaussian distributions in the case of larger climate shifts than model errors, based on distance

723 L_1 (top panel) and L_∞ (bottom panel). U refers to univariate correction, B to bivariate starting724 by variable 1 (12) or 2 (21) and H is for hypothesis H_{3-1} and V for hypothesis H_{3-2}

724



726 Figure 3: boxplots of the correction ratios obtained with 30 simulations with bivariate
 727 Gaussian distributions in both cases (larger model errors than climate shifts, top panel and
 728 larger climate shifts than model errors, bottom panel) based on distances $L1$ and $L\infty$ and for
 729 different correlation strengths between the variables: high (red), medium (orange) and low
 730 (blue). U refers to univariate correction, B to bivariate starting by variable 1 (12) or 2 (21) and
 731 H is for hypothesis H_{3-1} and V for hypothesis H_{3-2}

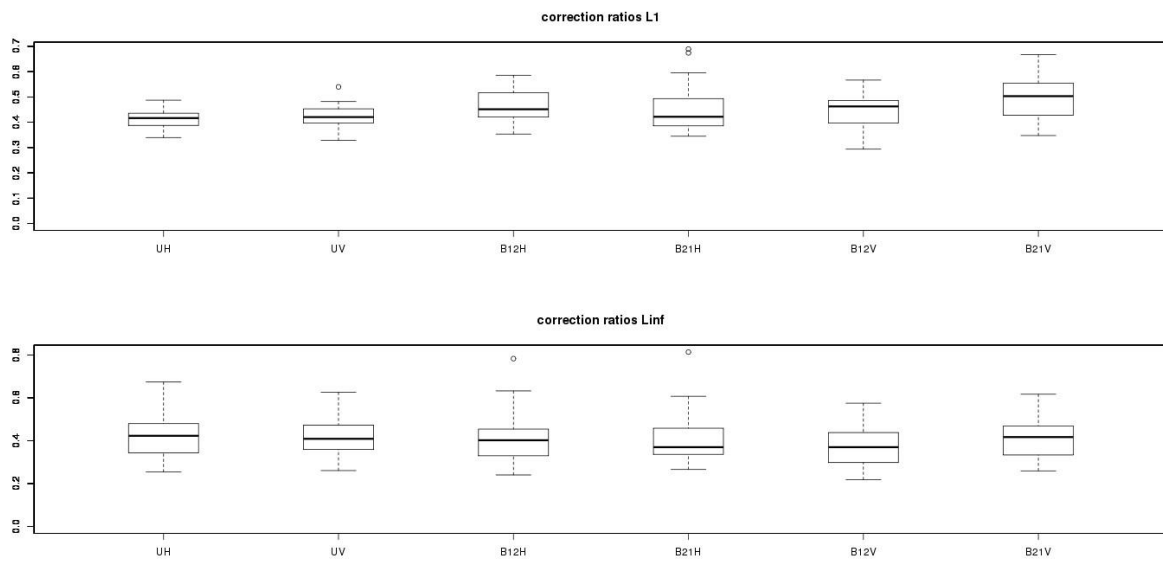


733 Figure 4: boxplots of the correlation coefficients obtained with 30 simulations with bivariate
 734 Gaussian distributions in both cases (larger model errors than climate shifts, top panel and
 735 larger climate shifts than model errors, bottom panel) and for different covariance strengths
 736 between the variables: high (red), medium (orange) and low (blue). Yf refers to the
 737 observations over the validation period, Xf to the simulation over the same period, U refers to
 738 univariate correction, B to bivariate starting by variable 1 (12) or 2 (21) and H is for
 739 hypothesis H_{3-1} and V for hypothesis H_{3-2}

740

741

742

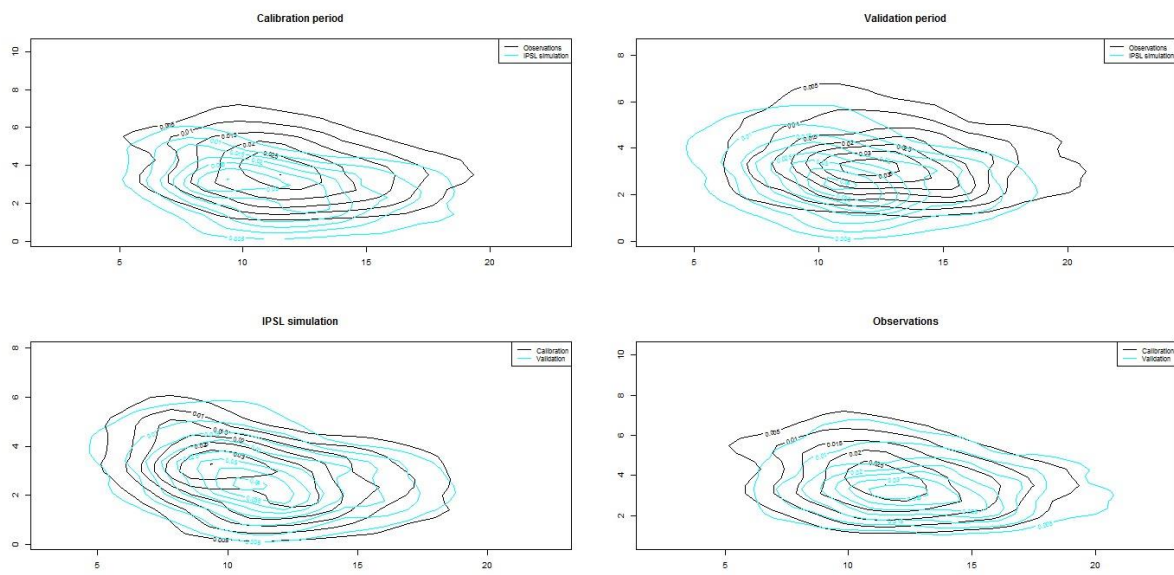


743

744 Figure 5: boxplots of the correction ratios obtained with 30 simulations with bivariate Gaussian
745 distributions in the case of moderate climate shifts and model errors, based on distance L_1 (top panel)
746 and L_∞ (bottom panel). U refers to univariate correction, B to bivariate starting by variable 1 (12) or 2
747 (21) and H is for hypothesis H_{3-1} and V for hypothesis H_{3-2}

748

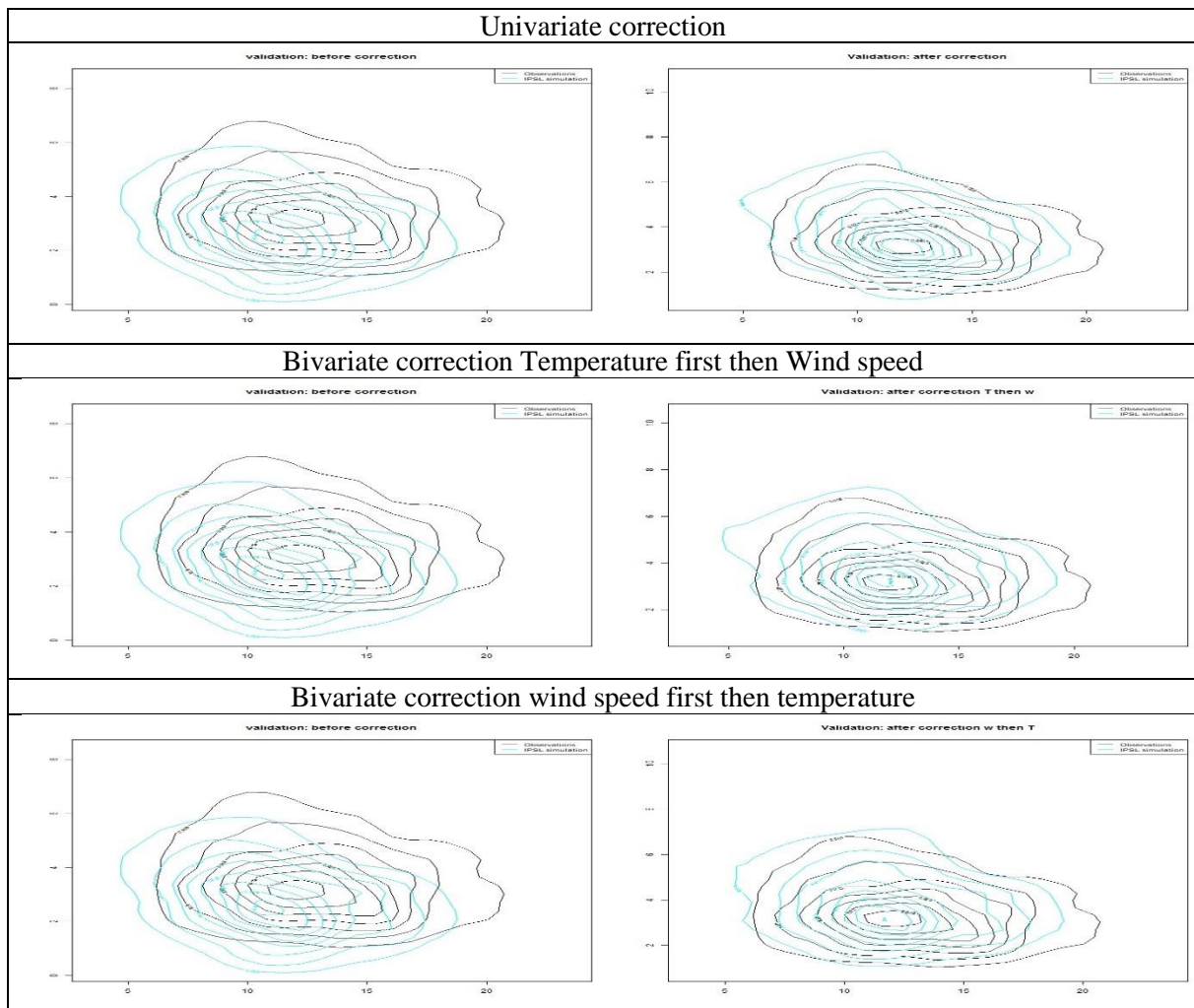
749



750

751 Figure 6: Top line: comparison between observed (black) and modeled (cyan) bivariate distributions
752 of temperature and wind speed in Hamburg for each period (calibration period: left panel, validation
753 period: right panel); bottom line: comparison between calibration (black) and validation (cyan)
754 bivariate distributions of temperature and wind speed in Hamburg for the model and the observations
755 (IPSL model: left panel; observations: right panel) for the month of May

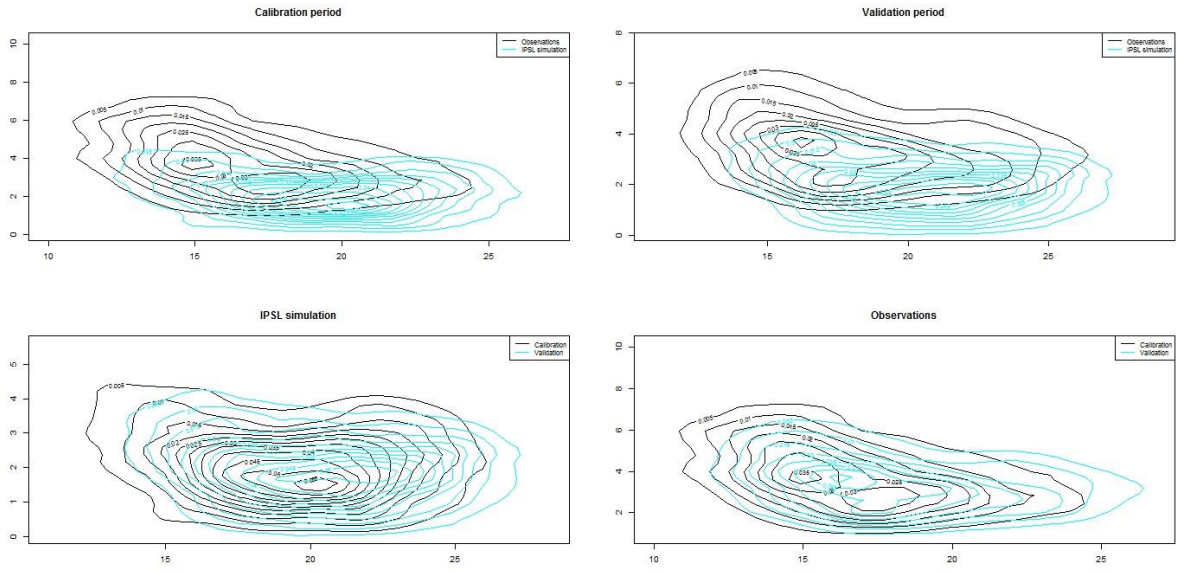
756



758 Figure 7: comparison between observed (black) and modeled (cyan) bivariate distributions of
 759 temperature and wind speed in Hamburg for the validation period before correction (left panels) and
 760 after univariate correction (top right), bivariate correction with temperature first (medium right) and
 761 wind speed first (bottom right) for the month of May

762

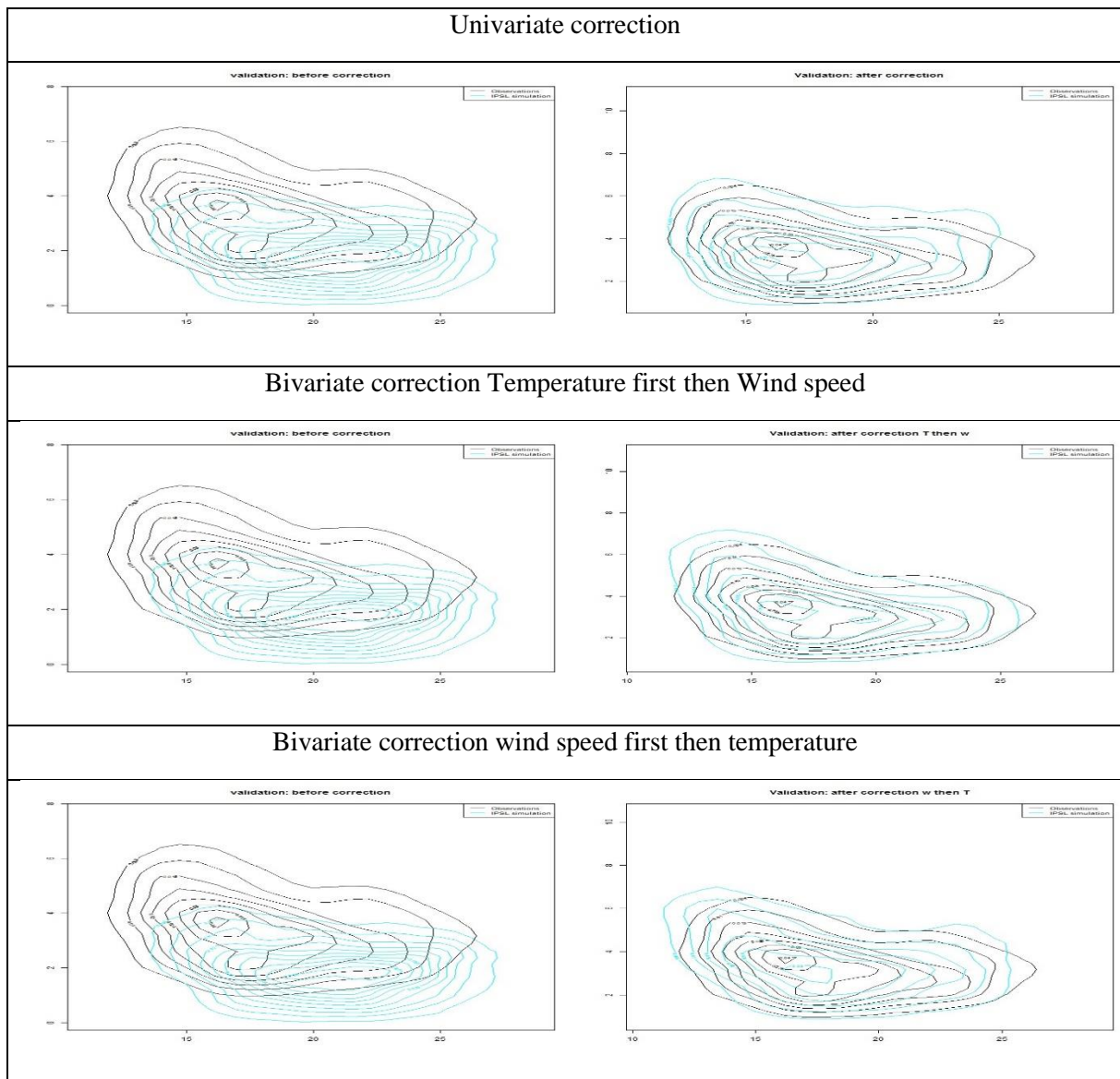
763



764

765 Figure 8: same as figure 6 but for the month of July

766



768 Figure 9: same as figure 7 but for the month of July